UNIVERSITÀ DEL PIEMONTE ORIENTALE

# UNIVERSITÀ DEGLI STUDI DEL PIEMONTE ORIENTALE "AMEDEO AVOGADRO"

**School of Medicine**

**Department of Health Sciences**

**Master's Degree in Medical Biotechnologies**

# Palmitate Amplifies the Pro-Atrophic Effects of AGEs Through Mitochondrial and Oxidative Stress-Related Alterations


*Supervisor:*

**Prof. Flavia Prodam**

*Co-supervisor:*

**Dr. Alessandro Antonioli**


Firmato digitalmente da Flavia Prodam
Data: 30.06.2026 21:00:53 CEST
Organizzazione: UNIVERSITA' DEGLI STUDI DEL PIEMONTE ORIENTALE/01943490027


*Candidate:*
**Rebecca David**
*Matricula number:* **20037942**


*Academic Year* 2025/2026

# *Table of Contents*

**Abstract** ..... 3

**Introduction** ..... 5

Sarcopenic Obesity ..... 6

Western Diet ..... 9

Aims of the project ..... 13

**Materials and methods** ..... 15

Cell cultures and treatments ..... 16

Reactive Oxygen Species (ROS) production ..... 16

RNA extraction and quantification of gene expression ..... 17

Western blotting ..... 17

TOM20 Immunofluorescence ..... 18

Bodipy ..... 18

Statistical Analysis ..... 18

**Results** ..... 19

Palmitate increased AGEs-induce C2C12 myotube atrophy ..... 20

Co-treatment of Palmitate and AGEs did not influence significantly catabolic systems ..... 21

PA and AGEs reduce mitochondrial content and promote oxidative stress in C2C12 myotubes ..... 23

**Discussion** ..... 27

**References** ..... 31

# Abstract

Sarcopenic obesity (SO), characterized by the coexistence of progressive skeletal muscle wasting and excessive adipose tissue accumulation, represents an increasingly prevalent condition in aging populations and is associated with impaired metabolic homeostasis and reduced functional capacity.. Among the dietary factors contributing to its pathophysiology, Western dietary patterns are of particular relevance, as they promote chronic exposure to saturated fatty acids, particularly palmitic acid (PA), together with the production and accumulation of advanced glycation end products (AGEs). Although lipotoxic and glycative stress coexist in SO, their combined effects on skeletal muscle and adipose tissue remain poorly characterized.

Building on previous findings from Prof. Riuzzi's laboratory (University of Perugia), showing that dietary AGEs induce myotube atrophy through distinct mechanisms, this thesis investigated firstly whether PA could amplify AGE-induced muscle wasting. Differentiated C2C12 myotubes, a well-established *in vitro* model for skeletal muscle studies, were exposed to PA, selected dietary AGEs, including methylglyoxal (MGO), carboxymethyl-lysine (CML), and pentosidine (PT), or their combination. Myotube diameter, expression of atrophy- and mitophagy-related genes, mitochondrial content, inflammatory signalling, and oxidative stress were evaluated. In parallel, differentiated 3T3-L1 adipocytes were used as a secondary preliminary model to assess whether AGEs could influence intracellular lipid accumulation.

Preliminary findings indicate that combined exposure to PA and dietary AGEs tends to induce greater myotube atrophy than either stimulus alone, accompanied by lower mitochondrial content and an increased accumulation of reactive oxygen species (ROS). In parallel, AGE treatments appeared to influence intracellular lipid accumulation in adipocytes in a time-dependent manner. Given the exploratory nature of these experiments, the findings require further validation.

Overall, these results support the hypothesis that Western diet-derived lipotoxic and glycative stress may contribute to the disruption of skeletal muscle and adipose tissue homeostasis in SO, providing a basis for future studies aimed at elucidating the molecular mechanisms underlying their interaction.

# Introduction

**Sarcopenic Obesity**

The term “sarcopenic obesity” (SO) was first introduced by Baumgartner to describe the coexistence of sarcopenia and obesity. [1] More specifically, this condition is characterized by a progressive loss of skeletal muscle mass occurring together with excessive ectopic fat deposition, particularly visceral fat, and with the accumulation of adipose tissue within muscles and organs such as the liver, heart, and pancreas. [2,3]

Although sarcopenia and obesity are considered distinct clinical conditions, they share several pathophysiological mechanisms and risk factors, including aging, sedentary lifestyle, endocrine alterations, increased production of inflammatory cytokines and reactive oxygen species. Rather than simply coexisting, these two conditions interact in a synergistic way, reinforcing one another and generating a detrimental vicious cycle. This process accelerates muscle wasting, chronic low-grade inflammation, oxidative stress, mitochondrial dysfunction and insulin resistance, ultimately leading to health complications that are more severe than those associated with either condition alone. [1,2,4]

Given the complexity of this condition, the development of standardized diagnostic criteria has become essential. For this reason, European Society for Clinical Nutrition and Metabolism (ESPEN) and the European Association for the Study of Obesity (EASO) proposed a standardized diagnostic consensus in 2022, introducing for the identification of SO a sequential three-step process, screening, diagnosis, and staging.

As reported in Donini et al, the first phase requires the simultaneous presence of a high BMI or increased waist circumference, both evaluated according to ethnicity-specific cut-off values, and the presence of surrogate indicators of sarcopenia, including clinical suspicion, symptoms or validated questionnaires. Only with a positive screening result, the diagnostic phase is then carried out. Once the diagnosis has been established, the final step is staging which is focused on the severity and progression of the disease. Two stages are recognized: stage I, characterized by the absence of complications, and stage II, defined by the presence of at least one complication related to SO, including metabolic diseases, functional disabilities or cardiovascular and respiratory disorders. [5]

Despite available evidence suggests that SO is relatively common among older adults, with prevalence estimates generally ranging between 9% and 14%, estimating the true prevalence of SO remains challenging, because studies still rely on heterogeneous diagnostic criteria and definitions. [4] A landmark meta-analysis including 50 studies and 86,285 individuals estimated a global prevalence of 11% among adults aged 60 years and older. Higher prevalence rates were observed in individuals aged over 75 years, hospitalized patients and South American and North American populations. No

substantial sex-related differences were identified, with prevalence estimates of 14% in women and 10% in men. [6]

Similar findings were reported by more recent systematic reviews and meta-analyses. One analysis including 71,757 non-hospitalized older adults reported a pooled prevalence of 14% (95% CI: 11–17%), while another broader review estimated an overall prevalence of approximately 9% in elderly populations. [7,8] Furthermore, population-based studies highlight that SO is strongly aged-related, with prevalence progressively increasing after 50 years and reaching 16.7% in individuals aged 80–89 years. [4]

Beyond its epidemiological burden, this condition underscores the key role of skeletal muscle in determining aging outcomes and survival, since impaired muscle function, particularly reduced strength and mass, has consistently emerged as an independent predictor of mortality, as recent meta-analysis confirmed that mortality risk is highest in patients with SO (HR 1.24, 95% CI 1.12–1.37) compared to healthy individuals, although the heterogeneity of diagnostic criteria was acknowledged as an important limitation. [9]

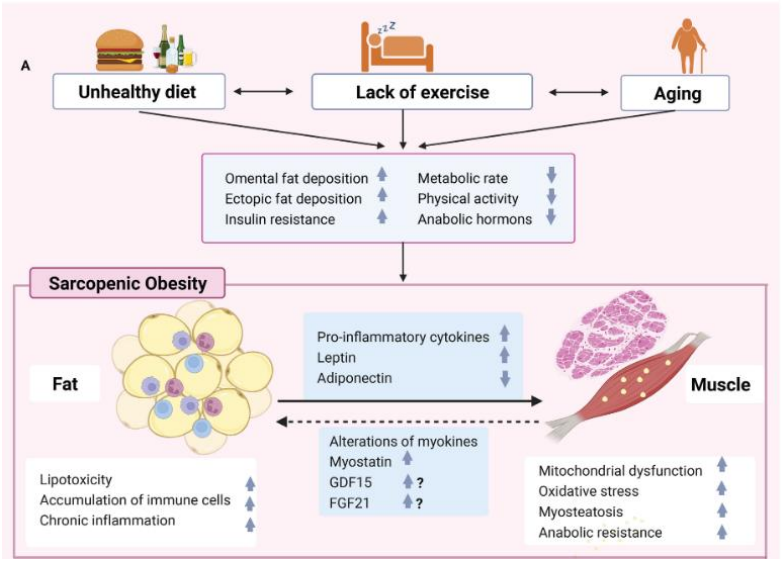


**Figure 1**: Pathophysiology and risk factors for sarcopenic obesity development. [4]

The detrimental vicious cycle that characterizes SO is sustained by specific molecular mechanisms, among which skeletal muscle atrophy and adipocyte hypertrophy play a central role.

Skeletal muscle accounts for approximately 40% of total body weight and represents a highly dynamic, heterogeneous and plastic tissue, whose primary roles are movement and support [10]. It is organized into fascicles containing multinucleated muscle fibers. These myofibers are composed of myofibrils arranged around the sarcomere, the fundamental contractile unit in which the interaction between actin and myosin enables muscle contraction and gives skeletal muscle its characteristic striated appearance. [11]

The entire muscle structure is supported by three connective tissue layers, epimysium, perimysium and endomysium, which surround respectively the whole muscle, individual fascicles and single myofibers. These structures ensure mechanical support, proper muscle function and provide pathways for blood vessels and nerves throughout the tissue. [12]

As previously mentioned, skeletal muscle is highly dynamic and its mass depends on the balance between protein synthesis and protein degradation, respectively anabolism and catabolism. Under physiological conditions, muscle homeostasis is maintained through a tightly regulated equilibrium between them. [2,13] However, this balance may be disrupted by several factors, including diet, hormones, physical activity, diseases and environmental or genetic factors [11]. In this condition, catabolic pathways overcome anabolic ones, leading to impaired protein synthesis, muscle loss and ultimately muscle atrophy. [14]

Atrophy is defined as a substantial reduction in skeletal muscle mass resulting from physiological conditions or systemic diseases. [15] This process progressively impairs muscle function and contributes to falls, debilitation, loss of independence and a reduced quality of life. [16,17] Muscle wasting results from an imbalance between protein synthesis and protein degradation. The regulation of protein synthesis is controlled by several anabolic pathways, among which the Akt/mammalian target of rapamycin (mTOR) axis is one of the most extensively studied. In this pathway, activation of the serine/threonine kinase Akt promotes mTOR signaling, thereby supporting protein synthesis and muscle maintenance. [18–20] Conversely, under catabolic conditions, proteolytic pathways become predominant, leading to enhanced protein degradation mainly through two major systems: the ubiquitin-proteasome system (UPS) and the autophagy-lysosome system. [15,21] The UPS becomes activated when muscle-specific E3 ubiquitin ligases, particularly atrogin-1/MAFbx and MuRF1, are overexpressed. Several studies conducted in both rodent models and cancer patients have shown that activation of the ubiquitin-proteasome system significantly contributes to muscle wasting, supporting its role as one of the main regulators of muscle atrophy. Together with the autophagy-lysosome pathway and mitophagy, which are essential for protein turnover, autophagosome formation, and the selective clearance of damaged organelles and dysfunctional mitochondria, this proteolytic system

plays a central role in the catabolic remodelling of skeletal muscle. Moreover, mitochondrial dysfunction itself represents an additional driver of muscle atrophy, as impaired mitochondrial quality control, reduced oxidative capacity, and altered energy homeostasis can further contribute to skeletal muscle degeneration. [21,22]

When skeletal muscle atrophy persists over time, it progressively impairs muscle performance and may ultimately contribute to the development of sarcopenia; in the context of SO, muscle wasting occurs alongside adipose tissue dysfunction, highlighting the central role of both skeletal muscle, as an endocrine organ involved in metabolic homeostasis, and adipose tissue in shaping its pathophysiology. [23]Adipose tissue is a metabolically active organ, classified into white adipose tissue (WAT), which stores energy, brown adipose tissue (BAT), which dissipates energy as heat, and beige adipose tissue, which can develop within WAT in response to stimuli such as exercise or cold exposure [24,25] In SO, adipocyte hypertrophy reduced the production of anti-inflammatory and insulin-sensitizing adipokines, especially adiponectin at the expense of pro-inflammatory cytokines such as leptin, TNF-α, IL-6, and IL-1β increases substantially. [26] Thus, exacerbation of myokine/adipokine profile contributes to muscle decline, adipose tissue dysfunction, and the synergic effect of sarcopenia and obesity [27] [28]

Although aging is a major driver of sarcopenia, its progression can be further exacerbated by physical inactivity, inadequate nutrition, neurodegenerative disorders, and chronic inflammation. [29]Among these modifiable determinants, diet plays a particularly relevant role in the onset, development, and progression of SO, providing a rationale to investigate how specific dietary patterns, especially Western diets, may contribute to the combined deterioration of skeletal muscle and adipose tissue metabolism [30]

**Western Diet**

The Western diet (WD) is a modern dietary pattern very common in highly industrialized nations, where economic development, mass food production and urban lifestyles created the conditions for this dietary pattern to emerge and consolidate. [31] The countries in which this dietary pattern is most prevalent are, for example, Iceland, Switzerland, the United States, Australia, Sweden, Germany and Denmark. [32]

It is characterized by high consumption of processed and refined foods, red and processed meats, added sugars and saturated and trans fats, with a low intake of fruits, vegetables, whole grains and nuts [32] These are products that have undergone significant industrial transformation from their natural state, with the intention to extend their shelf life or to enhance their flavour profile. As a result, this

unbalanced diet contains high-energy intake, with an overabundance of simple sugars and sodium, lacking supply of fibers, vitamins, and minerals, whose levels consumed are below recommendation. [33] Low intakes of these have been linked to an increased risk of chronic diseases such as obesity, type 2 diabetes, cardiovascular disease and several cancers. [34]

Among the components of the WD, particular attention has been given to saturated fatty acids, especially palmitic acid (PA, C16:0), one of the most abundant saturated fatty acids in nature, present in both animal and plant food sources. [35,36] Upon WD consumption, PA represents the predominant saturated fatty acid, accounting for approximately 55% of total dietary saturated fatty acid intake and comprising about 20-30% of the ones in membrane phospholipids and triglycerides. [37] The average dietary intake of PA is estimated at around 20-30 g/day, representing approximately 8-10% of total energy intake, with levels of 20-30% in animal lipids and 10-45% in vegetable oils. [36] PA is derived both from dietary fat and through endogenous synthesis via *de novo* lipogenesis from excess carbohydrate and protein intake. [37]Chronic exposure to elevated levels of PA has been associated with significant metabolic disturbances, including insulin resistance, dyslipidemia and increased ectopic fat accumulation, effects that are largely mediated through the activation of inflammatory pathways and endoplasmic reticulum stress. [38]

Moreover, WD is widely demonstrate to play a pivotal role in contributing to advanced glycation end-product (AGE) accumulation, both through the direct consumption of AGE-rich processed foods and through the chronic metabolic imbalances, particularly hyperglycemia and oxidative stress, that this dietary pattern promotes endogenously. [39,40] AGEs are heterogeneous class of molecules arising from the non-enzymatic interaction of glucose or other sugars with proteins or lipids. [41] They are formed through a complex, multi-step process known as the Maillard reaction. This reaction occurs when the free amino groups of proteins react with the carbonyl groups of reducing sugars, such as glucose, without the involvement of enzymes. [42]

AGEs can be either exogenous or synthesized endogenously within the body. [43] As mentioned before, exogenous AGEs derived upon WD consumption. In addition, the preparation and processing methods commonly employed in this diet, such as grilling, frying, heating and dehydration, substantially increase the dietary AGE content (dAGE). [39] The rising consumption of processed foods in modern society is leading to a continuous increase in AGE production and accumulation, representing a potential risk to human health.[44] After absorption by the gastrointestinal tract, these compounds are only partially eliminated through urinary excretion, resulting in their accumulation across multiple tissues. [39] To measure dAGE accumulation in the body, scientists typically track the levels of three key markers: MGO, CML and PENT. MGO is a highly reactive carbonyl compound

that acts as a key precursor in the formation of AGEs. Among the AGEs it generates, MG-H1 and CML are fluorescent in nature, while pentosidine (PENT) is non-fluorescent. [44]

| Products | AGE [1] (kU/100 g) | Products | AGE (kU/100 g) |
|---|---|---|---|
| Meats | | Carbohydrates | |
| Beef, raw | 707 | Bread, pita | 53 |
| Beef, steak, pan fried with olive oil | 10,058 | Bread, Greek, hard, toasted | 607 |
| Chicken, breast, skinless, raw | 769 | Biscuit (McDonald's) | 1470 |
| Chicken, boiled with lemon | 957 | Cookie, biscotti, vanilla almond | 3220 |
| Chicken, breast, breaded, deep-fried, 20 min | 9722 | Donut, chocolate iced, crème filled | 1803 |
| Chicken, skin, back or thigh, roasted, barbequed | 18,520 | Apple, baked | 43 |
| Chicken, skin, thigh, roasted | 11,149 | Apple, Macintosh | 13 |
| Turkey, ground, raw | 4957 | Fig, dried | 2663 |
| Turkey, ground, grilled, crust | 6351 | Carrots, canned | 10 |
| Bacon, fried, 5 min, no added oil | 91,577 | Tomato | 23 |
| Bacon, microwaved, 2 slices, 3 min | 9023 | Vegetables, grilled (broccoli, carrots, celery) | 226 |
| Lamb, leg, raw | 826 | Honey | 7 |
| Lamb, leg, broiled, 450°F, 1 min | 2431 | Fats | |
| Fish | | Almonds, roasted | 6650 |
| Salmon, fillet, microwaved | 912 | Butter, whipped | 26,480 |
| Salmon, fillet, broiled | 3347 | Margarine, tub | 17,520 |
| Trout, raw | 783 | Walnuts, roasted | 7887 |
| Trout, baked, 25 min | 2138 | Eggs | |
| Liquids | | Egg white, large, 12 min | 63 |
| Milk, whole (4% fat) | 5 | Egg yolk, large, 12 min | 1680 |
| Juice, apple | 2 | Egg, omelet, pan, low, butter, 13 min | 507 |

**Figure 2:** The dietary AGE content in food [44]

On the other hand, endogenous AGEs are typically formed in all tissues and body fluids under physiological conditions not only through the same non-enzymatic reactions involved in exogenous formation, but also through metabolic pathways such as glycolysis and the polyol pathway. During the breakdown of glucose or fructose, reactive molecules like glyceraldehyde and methylglyoxal are produced, which can then lead to AGE formation in hyperglycemia, oxidative stress and aging conditions. [42,43]

Both exogenous and endogenous AGEs can bind to their receptor, known as RAGE (Receptor for Advanced Glycation End-products), a multi-ligand trans-membrane protein belonging to the immunoglobulin superfamily. [45] This interaction plays a central role in the pathophysiology of several diseases and triggers the activation of multiple intracellular signalling pathways. As Muthyalaiah study demonstrated, AGE-RAGE axis drives NADPH oxidase activation, ROS accumulation and subsequent activation of NF-κB signalling, which upregulates RAGE expression, creating a positive feedback loop that sustains and amplifies cellular damage.[46] The resulted inflammatory condition activates downstream signalling cascades, including MAPK and the JAK-STAT pathway. In particular, STAT3 activation cooperates with NF-κB in amplifying the pro-inflammatory response. [47] In addition, AGEs sustain autophagy via RAGE-dependent signalling: on one hand, by reducing

mTOR phosphorylation, they prevent its suppressive action on autophagy; on the other, by stabilizing the Beclin-1/VPS34 complex, they actively promote the formation of autophagosomes. [48]

The downstream effects of AGE-RAGE axis activation, including oxidative stress, chronic inflammation and autophagy dysregulation, converge on skeletal muscle tissue, making it vulnerable to AGE-induced damage. Both endogenous and exogenous AGEs have been shown to induce skeletal muscle atrophy. In the context of endogenous AGEs, their accumulation activates RAGE leading to a downregulation of both AMPK and Akt, which has been implicated as a negative mediator of muscle mass by increasing protein degradation via the ubiquitin-proteasome system and a lower expression of myogenin and myosin-heavy chain (MHC), both essential for muscle maintenance and differentiation. [49] In vitro studies demonstrated that both common dAGEs and their precursor methylglyoxal (MGO) induce C2C12 myotube atrophy through ROS production, mitochondrial dysfunction, mitophagy, UPS activation and inhibition of myogenic potential, with ROS identified as the primary driver of atrophy regardless of AGE origin. [39] Notably, while AGE-BSA activates the RAGE-myogenin axis and reduces anabolic mTOR signaling, MGO induces glycolytic stress and STAT3 activation through a RAGE-independent mechanism, suggesting that dAGEs promote muscle wasting through multiple and partially distinct molecular pathways. [39]

Although the effects of AGEs on skeletal muscle have been relatively well characterized, their impact on adipose tissue remains less thoroughly investigated, and the underlying mechanisms are not yet fully elucidated. [50] Nevertheless, available evidence suggests that the AGE-RAGE axis plays a role in adipose tissue dysfunction, particularly in the context of obesity. The accumulation of AGEs in the extracellular matrix of adipose tissue has been shown to impair adipocyte differentiation, metabolism, and secretory activity through RAGE-dependent signalling pathways, leading to alterations in adipokine secretion that may predispose to insulin resistance.[51] At the cellular level, AGE-modified extracellular matrix has been shown to inhibit insulin-stimulated glucose uptake in adipocytes, an effect largely mediated by an increase in intracellular ROS generation. [50,52] *In vivo* studies further support the involvement of the AGE-RAGE axis in adipose tissue dysfunction, as RAGE-deficient mice fed a high-fat diet displayed improved insulin sensitivity, reduced adipose tissue mass, and an improved inflammatory profile compared to wild-type controls. [53] However, further research is needed to fully clarify the role of AGEs in adipose tissue biology and to determine the extent to which these mechanisms operate in humans under physiological and pathological conditions.

**Aims of the project**

Building on these evidences, preliminary findings from the laboratory of Professor Francesca Riuzzi (University of Perugia) demonstrated that both endogenous AGE-BSA and the dietary AGE precursor methylglyoxal (MGO) induce a dose-dependent reduction in myotube area and MyHC-II expression in C2C12 cells, accompanied by increased expression of the atrogenes Fbxo32 and Trim63. [39] Primarily, AGE-BSA and MGO appeared to act through distinct molecular mechanisms, involving the RAGE–myogenin axis and glycative stress with STAT3 activation. Then, the dietary AGEs carboxymethyl-lysine (CML) and pentosidine (PT) similarly reduced myotube area, although their mechanisms were not further investigated. [39]

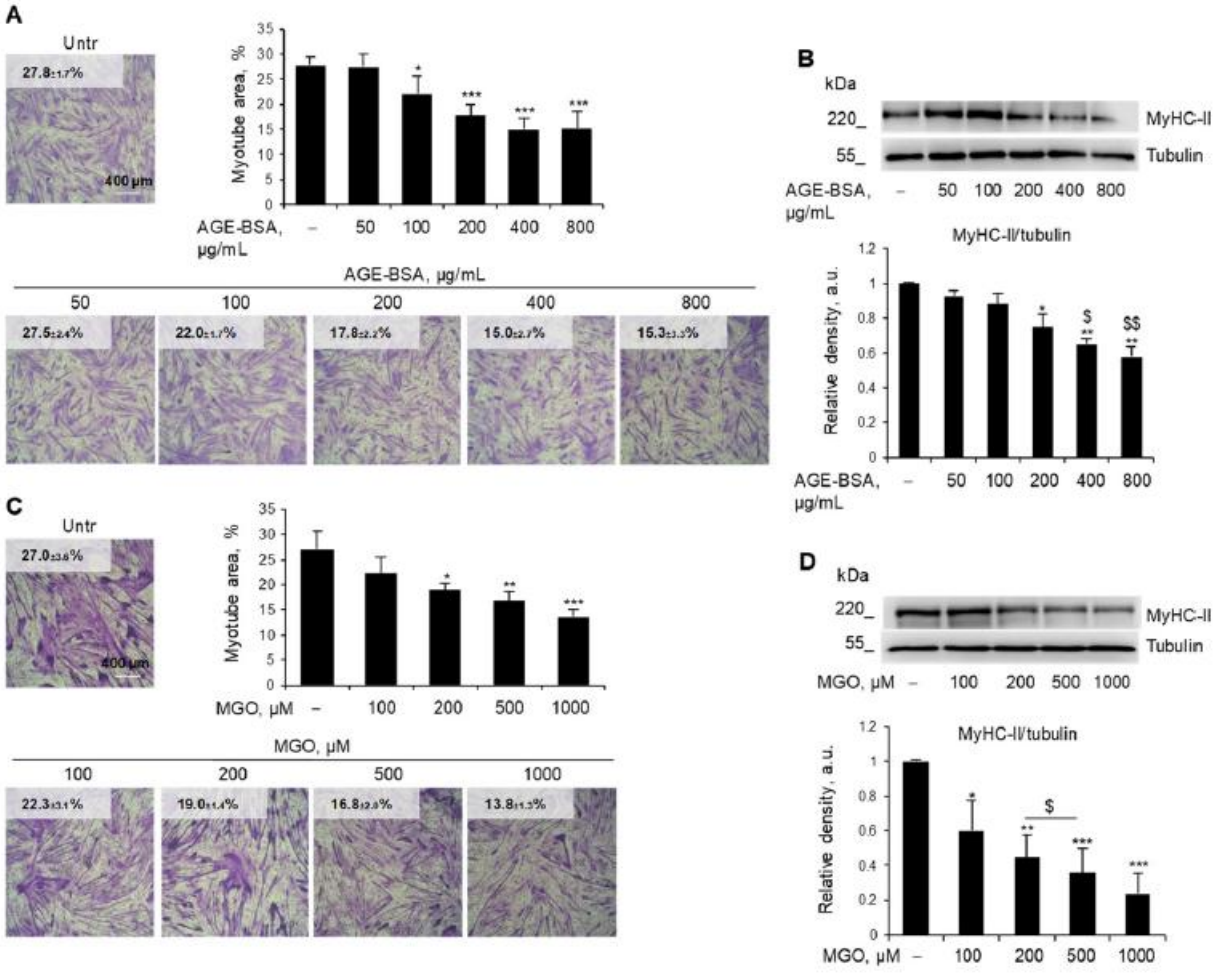


**Figure 3:** Endogenous and exogenous AGEs reduced myotube area and MyHC-II expression via partially distinct mechanisms (**A, C**). Myosin heavy chain (MyHC)-II expression was evaluated by Western blotting (WB) analysis, and the relative densities with respect to tubulin were determined (**B**, **D**). The expression of the atrogenes Fbxo32 and Trim63 (**E**) were assessed by real-time PCR, using Gapdh or Gusb as housekeeping genes (Paiella)

Given that sarcopenic obesity is associated with increased circulating palmitate (PA) levels and the accumulation of advanced glycation end-products (AGEs), the combined impact of these factors on

skeletal muscle remains poorly characterized. Therefore, this thesis project primarily aimed to investigate the effects of AGEs and PA, either alone or in combination, on skeletal muscle cells, with particular attention to whether the presence of PA was necessary and sufficient to exacerbate the atrophic effects induced by AGEs alone.

As a first experimental task, immortalized murine C2C12 myoblasts were differentiated into myotubes, one the most widely established and commonly used *in vitro* model to mimic skeletal muscle tissue[54]. In this system, the effects of PA were evaluated both individually and in combination with selected dietary AGEs, including carboxymethyl-lysine (CML), pentosidine (PT), and methylglyoxal (MGO), in order to assess their contribution to muscle wasting and the underling mechanisms.

As a secondary and preliminary objective, the same treatment conditions were also tested in differentiated 3T3-L1 adipocytes. Although this part of the project is still at an early stage and only preliminary data are available, this approach was designed to explore whether AGEs promote lipid accumulation in adipocytes and whether this effect is further enhanced by the concomitant presence of PA.

# Materials and methods

**Cell cultures and treatments**

C2C12 myoblasts (ECACC) were grown at low density in Dulbecco's Modified Eagle Medium (DMEM, Gibco, Thermo-Fisher Scientific) supplemented with 10% fetal bovine serum (FBS, Gibco, Thermo Fisher Scientific), 100 U/mL penicillin, 100 µg/mL streptomycin, and 0.25 µg/mL antimycotic in a humidified 5% CO2 incubator at 37°C.

To induce differentiation, cells were allowed to become confluent, and the medium was switched to differentiation medium (DM), consisting of DMEM supplemented with 2% horse serum (2%HS, GE Healthcare BioSciences), penicillin, streptomycin, and antimycotic as described above.

To obtain serum-free medium containing 2% fatty acid-free BSA, 0.5 g of BSA (Sigma A8806-5G) and 500 µL of horse serum were dissolved in 25 mL of 0% DMEM. Palmitate, from a 100 mM stock solution, was conjugated with the medium to reach a final working concentration of 200 µM or 500 µM, and incubated for 1 hour at 37°C. After conjugation, AGEs were added to the medium: MGO at a working concentration of 500 µM, CML at 400 µM and PT at 2 µM. Myotubes, after at least 5 days of differentiation, were then treated with this medium containing AGEs, palmitate, or the combination of both for 24 or 48 hours.

For every experiment were measured at least 10 myotubes diameter for each field, five different fields for each replicate, and three technical replicates for each used treatment. Myotubes diameters were measured with *JMicroVision* software.

3T3-L1 pre-adipocytes were grown at low density in Dulbecco's Modified Eagle Medium (DMEM, Gibco, Thermo Fisher Scientific) supplemented with 10% fetal bovine serum (FBS, Gibco, Thermo Fisher Scientific), 100 U/mL penicillin, 100 µg/mL streptomycin, and 0.25 µg/mL antimycotic in a humidified 5% $CO_2$ incubator at 37°C. To induce differentiation, cells were seeded and maintained in the same growth medium, which was replaced every 3 days until full differentiation was achieved at day 7. Medium for treatment was prepared as described above and fully differentiated 3T3-L1 adipocytes (day 7) were treated with the indicated AGEs at the same concentration for 24 or 48 h.

**Reactive Oxygen Species (ROS) production**

To measure cellular ROS production, C2C12 myotubes were stained with CellROX R Deep Red Reagent (Thermo Fisher Scientific; C10491) for 30 min at 37°C and washed with PBS. Fluorescent images were taken using the fluorescence microscope EVOS™ XL Core Imaging System, and the

mean fluorescence signal intensity was measured using ImageJ. For every experiment assessing cellular oxidative stress, at least three myotubes in each field, five different fields for each replicate, three technical replicates for each treatment were measured. The final data are the average of three independent experiments.

**RNA extraction and quantification of gene expression**

C2C12 myotubes were lysed using Nucleozol (Macherey Nagel) and after RNA extraction, the obtained RNA was retrotranscribed with high-capacity cDNA reverse transcription kit (Applied Biosystems, Thermo Fisher Scientific) and quantitative PCR (qPCR) was performed with StepOnePlus Real-time PCR System (Applied Biosystems, Thermo Fisher Scientific) using the following TaqMan probes (Thermo Fisher Scientific, Waltham, MA, USA): Fbxo32 (Mm00499523_m1), Trim63 (Mm01185221_m1), Gusb (Mm01197698_m1), Bnip3 (Mm01275600_g1), IL6 (Mm00446190_m1).

**Western blotting**

At the end of the treatments, cells were washed in ice-cold phosphate-buffer saline (PBS) and solubilized with a lysis buffer containing 1% Triton X-100, 0.1% sodium deoxycholate, 0.1% sodium dodecyl sulfate (SDS), 1 mM EDTA, 1 mM EGTA, 50 mM NaF, 160 mM NaCl, 20 mM Tris-HCl, pH 7.4, and supplemented with protease inhibitor cocktail.

Lysates were stirred for 1 minutes at 4°C and centrifuged at 15,000 × *g* for 15 min at 4° C. The concentration of proteins was determined by BCA protein assay kit. Proteins were resuspended in sample buffer containing 2% SDS, 150 mM dithiothreitol (DTT), and 0.01% bromophenol blue, and 40 µg protein/lane were separated by 6% SDS-PAGE and transferred to PVDF.

Membranes were saturated with 4% BSA, probed with the primary antibodies overnight at 4 °C, washed with tris-buffered saline (TBS) 0.1% Tween, incubated with the appropriate secondary antibody for 1 hour at room temperature, visualized with Western Lightning Chemiluminescence Reagent Plus (Perkin Elmer Life and Analytical Sciences), acquired with ChemiDoc Touch (Bio-Rad) and analysed with ImageLab (Bio-Rad).

**TOM20 Immunofluorescence**

Cells were seeded on sterile glass coverslips and washed with 1X PBS. Samples were fixed with 4% PFA in 1X PBS for 10 minutes at room temperature, then rinsed three times with 1X PBS, 5 minutes each. Permeabilization was carried out by incubating with 0.2% Triton X-100 in 1X PBS for 5 minutes at room temperature, followed by three additional 1X PBS washes of 3 minutes each. Non-specific binding was blocked by incubating with blocking buffer for 1 hour at room temperature.

After aspirating the blocking buffer, samples were incubated with TOM20 (Proteintech 11802-1-AP) for 2 hours at room temperature or overnight at 4°C. Following three washes with 1X PBS for 5 minutes each, samples were incubated with the fluorochrome-labeled secondary antibody diluted in antibody dilution buffer. A final series of three washes with 1X PBS for 3 minutes each was performed. Coverslips were then mounted and sealed, and the target antigen was visualized using a fluorescent microscope.

**Bodipy**

To measure the production of lipid droplets, adipocytes were fixed in 4% PFA for 10 minutes, washed with ice-cold phosphate-buffer saline (PBS), incubated for 30 minutes with Bodi-PY at RT and washed again with PBS. Images were taken using EVOS™ XL Core Imaging System, and the mean fluorescence signal intensity was measured using ImageJ.

**Statistical Analysis**

Data were first analyzed with Microsoft Excel to calculate mean and outliers. Outliers in the measurement were identified by mean of the interquartile range (IQR), as either below Q1−1.5 IQR or above Q3+1.5 IQR and excluded from the analysis. Statistical analysis and graphs were created using GraphPad Prism 8 program and groups variation was determined through student's t-test or ANOVA test. Data are presented as mean ± standard error of the mean (S.E.M.), with significance set as * $p < 0.05$, ** $p < 0.01$; ***$p<0.001$; ****$p<0.0001$.

# Results

**Palmitate increased AGEs-induce C2C12 myotube atrophy**

The first step in investigating the atrophic effect of palmitate (PA) was to evaluate the compound at different concentrations in order to identify a dose capable of inducing atrophy in C2C12 myotubes.

Although in the published article treatments were performed in differentiation medium, in our study treatments were carried out in serum-free medium containing 2% fatty acid-free BSA, to better mimic physiologic conditions and to avoid crystals formation. To this purpose, myotubes were treated with increasing concentrations of palmitate (PA: PA100 µM, PA200 µM, PA500 µM and PA750 µM) for 24 and 48 hours, using the widely demonstrated dexamethasone (DEXA) as a positive control of atrophy. [55] The effect of PA treatment on myotube diameter, a widely accepted morphological indicator of muscle atrophy, was then assessed.

Strikingly, despite low doses of PA did not reduce myotube diameter at the first timepoint, additional 24h were sufficient to reduce significantly myotube width. Meanwhile, as expected, higher doses of PA resulted in a greater reduction in myotube diameter at both 24 and 48 hours, confirming a dose-dependent relationship in the induction of muscle atrophy. The effect at 48h appears to be slightly more pronounced, with lower PA concentrations already inducing significant atrophy, and with PA500 and PA750 producing comparable reductions in myotube diameter.

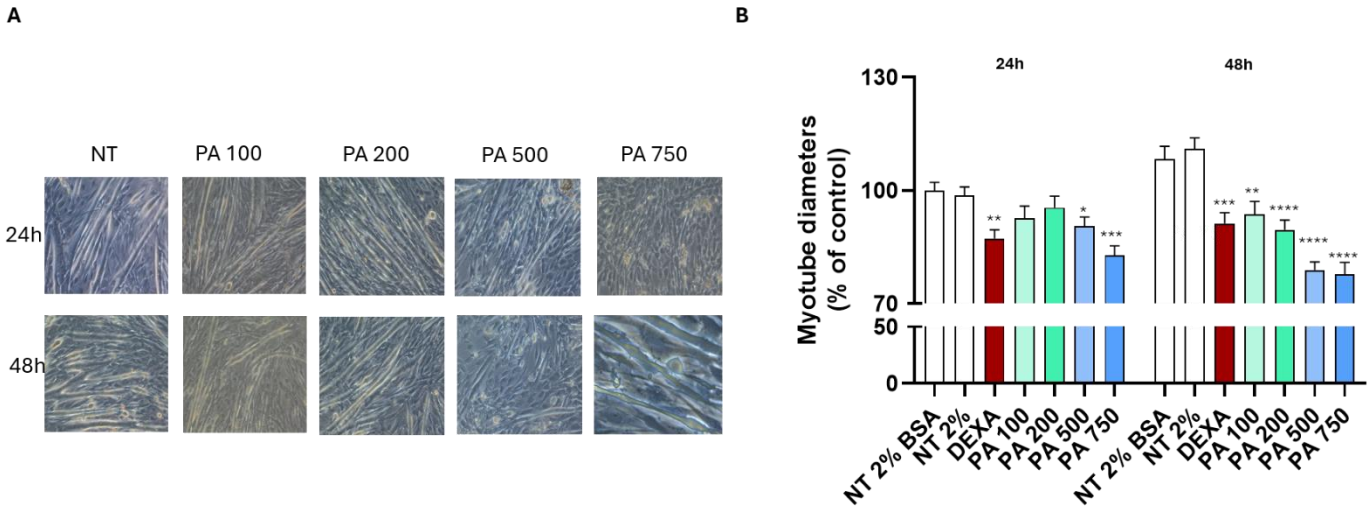


**Figure 4:** A reduction in myotube diameter was observed following PA treatment in a dose-dependent manner at both 24h and 48h time points. (**A, B).** Data are presented as mean ± standard error of the mean (S.E.M.) of at least three independent experiments. Data were analyzed using one-way ANOVA test ****P<0.0001 ***P<0.001 **P<0.01 *P<0.05 compared with NT 2% BSA of the relative timepoint.

Given these results, we selected for successive experiments at 24 and 48h PA500µM and PA 200µM respectively, since were observed to be the lowest dose sufficient in inducing a significant reduction of myotube diameter.

Based on Paiella results, to test whether PA could worsen AGEs-dependent atrophic effect in C2C12 myotubes, MGO (500 µM), CML (400 µM) and Pt (2 µM) were administered both alone and in combination with PA.

As is shown in the graph MGO, CML, and Pt alone significantly reduced myotube diameter in both the endpoints. Notably, the co-treatment of MGO or CML with PA generally exerted a greater reduction in diameter than either treatment alone particularly after 48h, supporting that the synergic effect on muscle atrophy could be time-dependent.

Nevertheless, Pt elicited a different pattern over time. Despite at 48 hours the trend is similar with MGO and CML, at 24 hours, myotube diameter in the PA+Pt group was not significantly different from non-treated myotubes (NT) and was higher than in the PA- or Pt-treated groups. Thus, unlike the other AGEs, Pt did not enhance the atrophic effect of PA at the earlier timepoint.

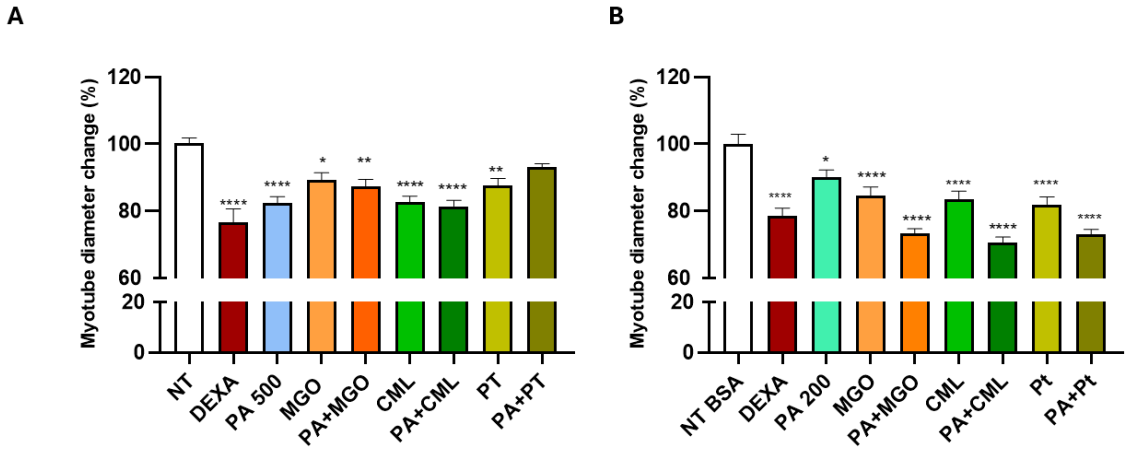


**Figure 5:** Myotube diameter reduction following treatment with AGEs (MGO 500 µM, CML 400 µM, Pt 2 µM), palmitate, and their combination, after 24h with PA500 µM (A) and 48h with PA200 µM (B). Data are presented as mean ± standard error of the mean (S.E.M.) of at least three independent experiments. Data were analysed using one-way ANOVA ****P<0.0001 **P<0.01 *P<0.05 compared with NT of the relative treatment.

**Co-treatment of Palmitate and AGEs did not influence significantly catabolic systems**

Since AGE-BSA and MGO have previously been shown to induce myotube atrophy through activation of the ubiquitin-proteasome system (UPS)[39], we next investigated whether this proteolytic

pathway was also involved in the response to PA, either alone or in combination with AGEs. To this end, we assessed the expression of the two main muscle-specific E3 ubiquitin ligases, Fbxo32 and Trim63. Fbxo32 mRNA expression was modestly increased by MGO, CML and Pt treatment alone, without further augmentation upon the treatment with PA200, despite the greater reduction in myotube diameter observed under the same combined conditions (Figure 5). PA200 alone did not increase Fbxo32 neither Trim63 expression, which remained substantially unchanged across all treatments, suggesting that the observed atrophy may not be induced by activation of atrogenes.

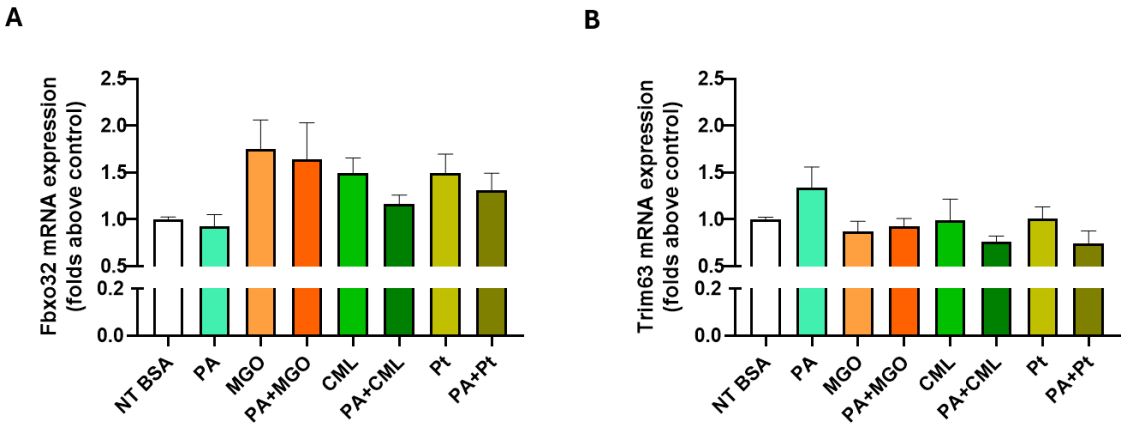


**Figure 6:** C2C12 myotubes were treated with PA 200 and MG 500 µM, CML 400 µM and Pt 2 µM for 24 h in 2% BSA FFA. (**A**, **B**) Real-time PCR analysis was performed to evaluate Trim63, Fbxo32 levels. Gene expression was normalized to Gusb. Data are presented as means ± standard error of the mean (S.E.M.) of two independent experiments.

Given the limited induction of them, we then investigated the putative autophagic/mitophagic mechanism. Differences among the conditions were not well appreciated in Bnip3 expression, with only minor variations across treatments, with PA200 displaying the highest mean value among all conditions tested. Combination treatments (PA+MGO, PA+CML, PA+Pt) did not show a consistent pattern relative to the corresponding AGE alone. None of these differences reached statistical significance. Notably, the different results obtained compared with the study by Paiella et al. pave the way to consider that the medium in which the treatments were performed may play a pivotal role in mitigating, modulating, or even reverting the observed outcomes.

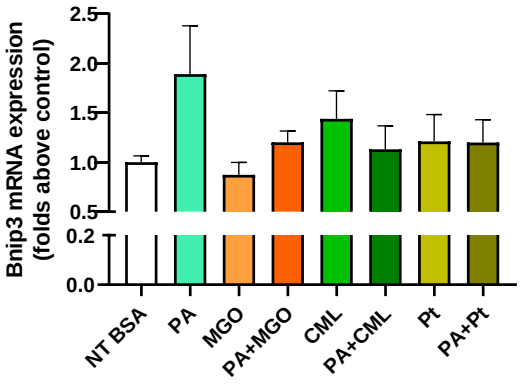


**Figure 7:** C2C12 myotubes were treated with PA 200 and MG 500, CML 400 and Pt 2 for 24 h in 2% BSA FFA. Real-time PCR analysis was performed to evaluate Bnip3 levels. Gene expression was normalized to Gusb. Data are presented as means ± standard error of the mean (S.E.M.) of two independent experiments.

**PA and AGEs reduce mitochondrial content and promote oxidative stress in C2C12 myotubes**

Considering the lack of changes in atrogenes and Bnip3 expression, we directly assessed mitochondrial content rather than relying on transcriptional markers of mitophagy, by performing TOM20 immunofluorescence. TOM20 mean fluorescence was reduced by all treatments compared to NT. Strikingly, PA, MGO, CML, and Pt alone induced a significant reduction in TOM20 signal, whose fluorescence was further decrease in the co-treatment PA-AGE, mirroring the trend observed for myotube diameter reduction.

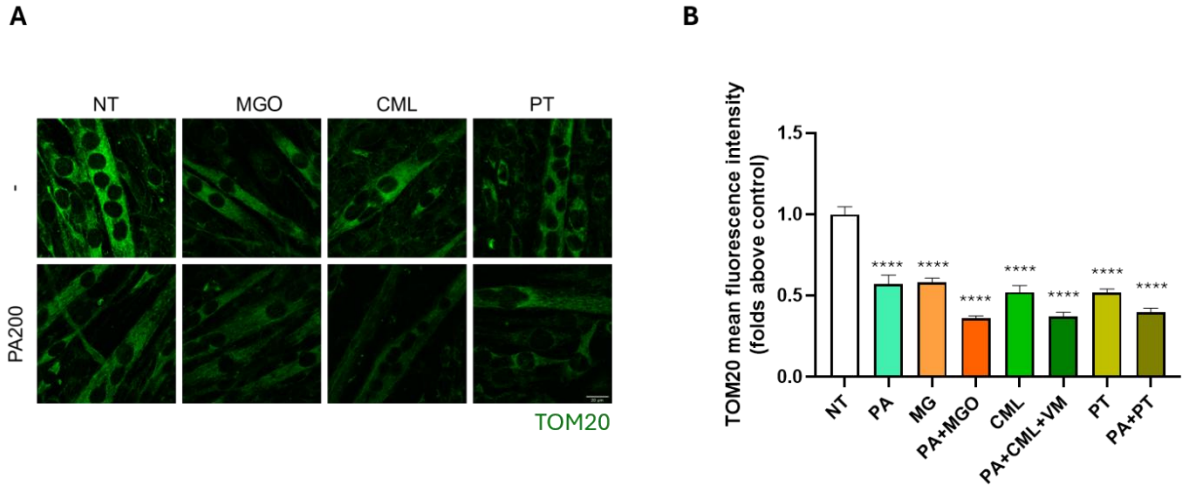


**Figure 8:** (A) Representative immunofluorescence images of TOM20 staining in C2C12 myotubes treated with PA200 and/or AGEs (MGO, CML, Pt) for 48h. Scale bar, 20 µm. (B) TOM20 mean fluorescence intensity was quantified and normalized to untreated control. Data are presented as mean ± S.E.M. of individual myotubes from a single experiment. Data were analysed using one-way ANOVA ****P<0.0001.

Following the more pronounced reduction in TOM20 fluorescence observed under combined treatment conditions and considering the central role of mitochondria as regulators of inflammatory processes [56], we delve into the investigation firstly of the activation of inflammation through qPCR analysis of IL-6 gene expression and then through reactive oxygen species (ROS) quantification and Western blot analysis of p-p38 to assess oxidative stress. PA alone, coherently to what observed in literature [57] induced a huge and statistically significant increase in IL-6 expression compared to untreated control, whereas AGEs alone did not affect its levels. Notably, combination treatments resulted in IL-6 levels markedly lower than those induced by PA alone, although still higher than those induced by the corresponding AGE alone.

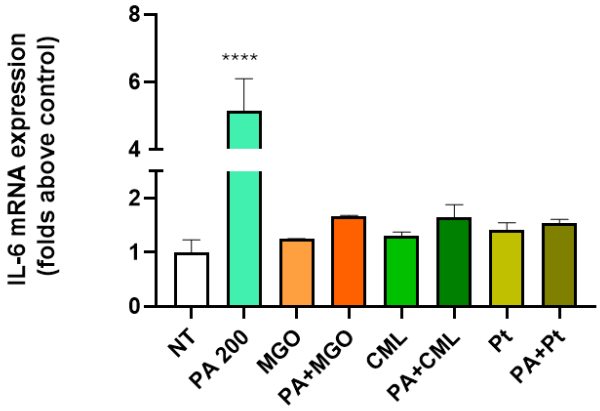


**Figure 9:** C2C12 myotubes were treated with PA 200 and MG 500, CML 400 and Pt 2 for 24 h in 2% BSA FFA. Real-time PCR analysis was performed to evaluate IL6 levels. Gene expression was normalized to Gusb. Data are presented as means ± standard error of the mean (S.E.M.) of three independent experiments. Data were analyzed using one-way ANOVA. ****P<0.0001.

In line with the previous finding, IL-6 high levels resulted in an elevation of ROS accumulation upon PA treatment, in presence or absence of AGEs. To gain this results ROS were evaluated through CellROX staining, with a significant increase among all the conditions suggesting an increased accumulation within C2C12 myotubes. Interestingly, although the data need to be validated with other experiments, we observed also an increase of p38 phosphorylation, as a confirmation of a putative oxidative stress condition.

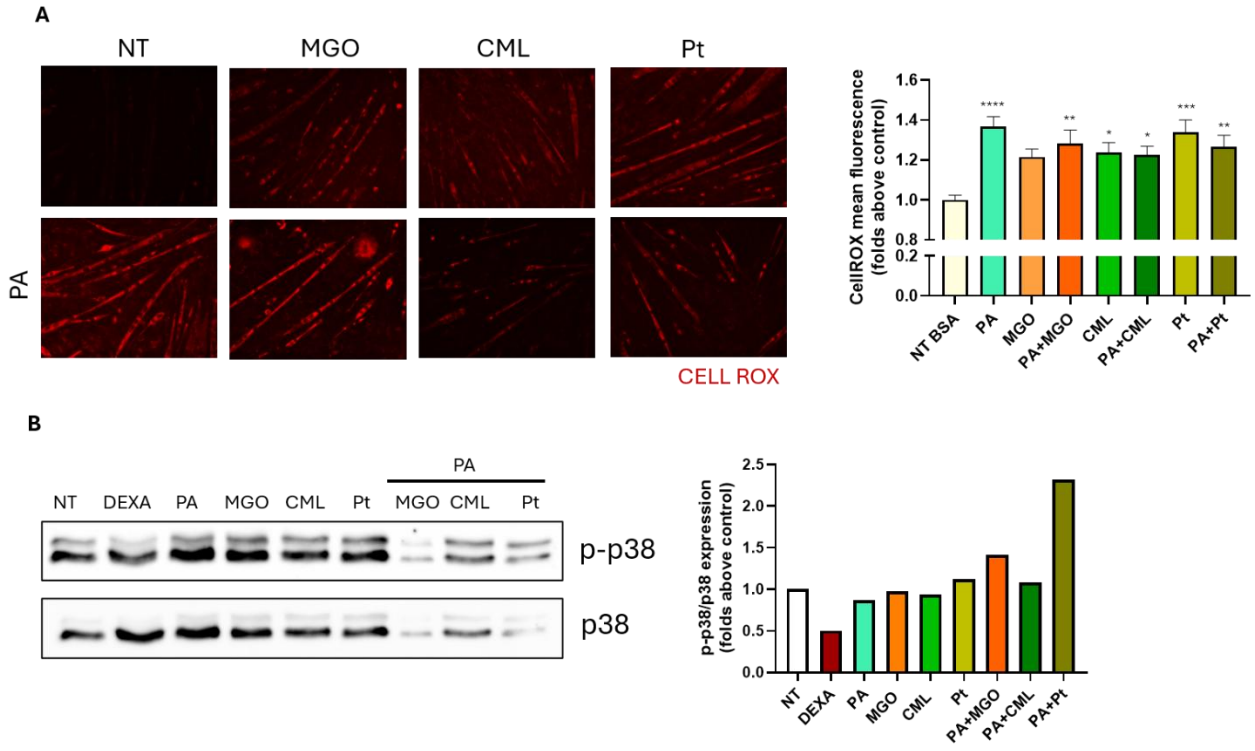


**Figure 11:** (**A**) Representative CellROX fluorescence images of C2C12 myotubes treated with PA200 and/or AGEs (MGO, CML, Pt) for 48h. CellROX mean fluorescence intensity was quantified and normalized to untreated control. H2O2 was used as a positive control (C+). Data are presented as means ± S.E.M. of two independent experiments. Data were analysed using one-way ANOVA ****P<0.0001 **P<0.01 *P<0.05 (**B**) p-p38 levels were evaluated through Westerb Blot analysis. P-p38 intensity was normalized on p-38 total. Data are presented as mean ± standard error of the mean (S.E.M.) of one indipendent experiment

To preliminarily assess whether AGEs affect not only skeletal muscle trophism and homeostasis, but also lipid metabolism in adipocytes, differentiated 3T3-L1 cells were exposed to the same treatment conditions with MGO (500 µM), CML (400 µM), and Pt (2 µM) for 24 and 48 hours. Neutral lipid accumulation was evaluated by BODIPY 493/503 staining.

Interestingly, AGEs increased lipid droplet accumulation already at the earliest time point analysed, with a further increase observed after 48 hours of treatment. These preliminary findings suggest that AGEs may directly influence lipid storage in adipocytes and provide the basis for further investigating if the concomitant addition of PA, which is already known to promote itself lipid droplet accumulation [58], may further exacerbate this effect.

Overall, these findings need to be fully validated to gain insights on the mechanisms that could play pivotal roles at the basis of SO.

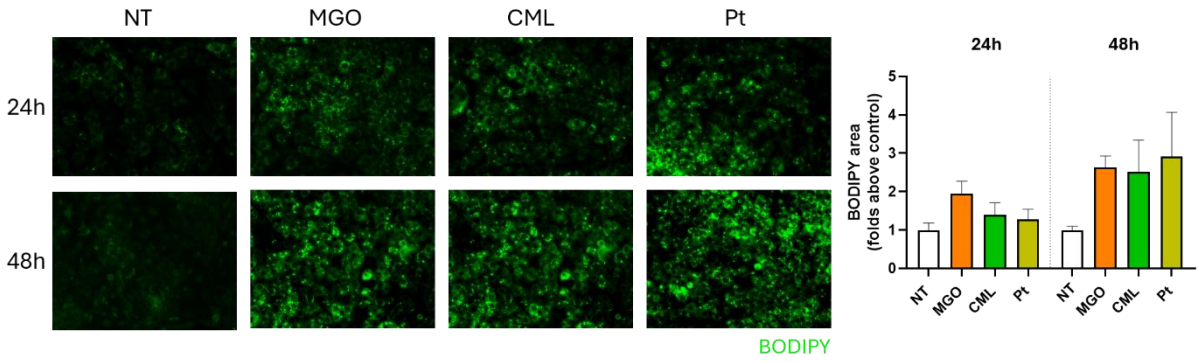


**Figure 12:** (**A**) Representative BODIPY fluorescence images of 3T3-L1 adipocytes treated with MGO, CML, and pentosidine (Pt) for 24h or 48h. (**B**) BODIPY mean fluorescence area was quantified and normalized to untreated control (NT). Data are presented as means ± S.E.M. of one independent experiments.

# Discussion

SO arises from a self-reinforcing interaction between skeletal muscle wasting and adipose tissue dysfunction, in which WD-derived factors, particularly PA and dietary AGEs (dAGEs), are increasingly recognized as contributing drivers. While dAGEs have previously been shown to induce myotube atrophy through RAGE-dependent and RAGE-independent mechanisms (Paiella), and elevated circulating PA is a hallmark of SO, had not been investigated until now whether these two factors interact in worsening muscle wasting. Therefore, this thesis aimed to determine the role of PA in modulating AGE-induced myotube atrophy, thereby extending the findings of Paiella et al. (2025). Thus, a combined dietary exposure model, representative of key components of the WD, was adopted. Differentiated C2C12 myotubes were used as the primary experimental model to assess skeletal muscle alterations, while differentiated 3T3-L1 adipocytes were included as a secondary and preliminary model to explore potential effects on adipocyte lipid metabolism.

Combined treatment of C2C12 myotubes with PA and dAGEs produced a greater reduction in myotube diameter than either stimulus alone, indicating that co-exposure to saturated fatty acids and exogenous AGEs exerts an additive atrophying effect. This observation supports the hypothesis that lipotoxic stress may potentiate AGE-induced skeletal muscle wasting, suggesting that the coexistence of glycative and lipid-related stressors, as occurs in WD-associated metabolic dysfunction, may exert a greater detrimental effect on muscle trophism than either stimulus alone.

Notably, the enhanced morphological atrophy was not accompanied by a proportional activation of the canonical transcriptional pathways previously linked to AGE-induced muscle wasting. Despite it is demonstrated that AGE-BSA and MGO stimulate the UPS through upregulation of Trim63 and Fbxo32 [39], in the present study the combined treatments failed to produce an additive increase in either atrogenes. Notably, PA did not affected their expression, coherently with de Hart study in which PA induced inflammation and myotube atrophy in C2C12 cells without interfering with atrogenes activation. [59]

Likewise, whereas MGO was previously shown to increase Bnip3 expression, neither MGO nor the other treatments significantly affected Bnip3 expression in our experimental conditions. Together, these findings indicate that the more pronounced atrophic phenotype cannot be readily explained by enhanced activation of the classical ubiquitin-proteasome or mitophagy-related transcriptional programs. However, these results should be interpreted in light of the different experimental conditions used compared with Paiella et al. In particular, while in the previous study the treatments were performed in differentiation medium, in the present work PA was conjugated and administered in a fatty acid-free BSA-containing medium, which more closely resembles the physiological transport of free fatty acids in biological fluids. This experimental condition may influence PA

bioavailability, cellular uptake, and cytotoxicity, potentially attenuating the activation of classical catabolic transcriptional responses. Therefore, differences in treatment medium composition may partially explain the discrepancy between the present findings and those previously reported.

Interestingly, although no differences were appreciated quantifying mitophagy activation, mitochondrial content emerged as the variable most closely associated with the morphological phenotype. Indeed, TOM20 fluorescence was reduced by both PA200 and each individual AGE, while combined treatments consistently produced a greater loss of signal, closely paralleling the reduction in myotube diameter. This association suggests that the reduction in TOM20 mean fluorescence, used as an indirect indicator of mitochondrial content, may contribute to the more pronounced atrophic phenotype observed under combined treatment conditions. Indeed, it is well established in the literature that mitochondrial dysfunction and inadequate mitochondrial turnover contribute to the development of skeletal muscle atrophy [60]. For this reason, the absence of significant changes in Bnip3 expression may indicate that mitochondrial turnover is not adequately activated despite the loss of mitochondrial signal, suggesting a potential dysregulation of mitochondrial quality control. This imbalance could contribute to the development of inflammatory signalling and oxidative stress, thereby promoting myotube atrophy.

Conversely, contrary to what was expected, AGEs, either alone or in combination with PA, induced only a modest and non-significant increase in IL-6 expression. Thus, although inflammatory signalling may contribute to the atrophic phenotype, these findings suggest that PA represents the main driver of Il-6 induction under the present experimental conditions.

Parallelly, since both inflammation and mitochondrial dysfunction are strictly correlated and recognised as primary sources of reactive oxygen species (ROS) production and accumulation [61], oxidative stress was evaluated measuring CellROX fluorescence. We observed that not only PA, but also AGEs treatments, either alone and in combination with PA, triggered cellular damage, as highlighted by the high production of ROS and by the higher phosphorylation of p38 protein, characteristic of an augmented oxidative stress condition [62]. Nevertheless, CellROX fluorescence provides a measure of total cellular ROS, without discrimination between mitochondrial and extra-mitochondrial sources of oxidative stress. Indeed, we planned to assess mitochondria-targeted probes or antioxidants, such as MitoSOX or mitoTEMPO to clarify whether mitochondrial dysfunction directly contributes to ROS production in this model.

In the present study dAGEs were administered individually or in combination with PA, whereas in a real dietary context multiple AGEs are typically present simultaneously; testing combinations of MGO, CML and Pt together, rather than separately, would provide an even more physiologically

relevant representation of WD-derived AGE exposure. Given the relatively modest effects observed at the doses tested, increasing AGE concentrations or the combination of them may also help to determine whether more pronounced or more consistent additive effects with PA can be achieved, particularly at the molecular level. In addition, the limited number of biological replicates currently available precludes firm conclusions, and these findings should therefore be considered preliminary until confirmed by additional experiments. More broadly, the present data suggest that the additive atrophic effect of PA and AGEs does not appear to be primarily mediated by the canonical catabolic and inflammatory pathways examined here, indicating that alternative or complementary mechanisms remain to be identified. Future work should aim to further dissect how PA modifies the cellular response to AGEs, for instance by exploring lipid-related stress pathways not addressed in the present study.

Finally, since Vaccinium macrocarpon (VM) was previously shown to counteract AGE-induced myotube atrophy (Paiella), it would be of particular interest to determine, at least morphologically, whether VM is also able to avoid or counteract atrophic phenotype induced by the combination of PA and AGEs, which may involve mechanisms distinct from those targeted by VM in the AGE-only model.

As a secondary and preliminary objective, the effect of AGEs on lipid accumulation was assessed in differentiated 3T3-L1 adipocytes using BODIPY staining suggesting a time-dependent accumulation of neutral lipids in response to AGE treatment, with effects becoming more consistent and pronounced at 48 hours. Collectively, these preliminary findings suggest that dAGEs promote intracellular neutral lipid accumulation in adipocytes in a time-dependent manner, pointing to a potential role of glycative stress in lipid metabolic dysregulation. However, given that PA was not included in this experimental set and that only a limited number of replicates are currently available, these data should be regarded as exploratory. Future investigations should incorporate PA co-treatment to determine whether lipotoxic and glycative stimuli act synergistically to dysregulate lipid metabolism in adipocytes, as would be expected in the metabolic context of SO. In addition, testing the simultaneous administration of multiple AGEs, rather than individual compounds, would provide a more physiologically relevant representation of WD-derived glycative exposure, mirroring the approach proposed for the C2C12 model.

# References

1. Wannamethee, S.G., and Atkins, J.L. (2015). Muscle loss and obesity: the health implications of sarcopenia and sarcopenic obesity. Proceedings of the Nutrition Society *74*, 405–412. https://doi.org/10.1017/S002966511500169X.

2. Bilski, J., Pierzchalski, P., Szczepanik, M., Bonior, J., and Zoladz, J.A. (2022). Multifactorial Mechanism of Sarcopenia and Sarcopenic Obesity. Role of Physical Exercise, Microbiota and Myokines. Cells *11*, 160. https://doi.org/10.3390/cells11010160.

3. Batsis, J.A., and Villareal, D.T. (2018). Sarcopenic obesity in older adults: aetiology, epidemiology and treatment strategies. Nat Rev Endocrinol *14*, 513–537. https://doi.org/10.1038/s41574-018-0062-9.

4. Wei, S., Nguyen, T.T., Zhang, Y., Ryu, D., and Gariani, K. (2023). Sarcopenic obesity: epidemiology, pathophysiology, cardiovascular disease, mortality, and management. Front. Endocrinol. *14*. https://doi.org/10.3389/fendo.2023.1185221.

5. Donini, L.M., Busetto, L., Bischoff, S.C., Cederholm, T., Ballesteros-Pomar, M.D., Batsis, J.A., Bauer, J.M., Boirie, Y., Cruz-Jentoft, A.J., Dicker, D., et al. (2022). Definition and Diagnostic Criteria for Sarcopenic Obesity: ESPEN and EASO Consensus Statement. Obes Facts *15*, 321–335. https://doi.org/10.1159/000521241.

6. Gao, Q., Mei, F., Shang, Y., Hu, K., Chen, F., Zhao, L., and Ma, B. (2021). Global prevalence of sarcopenic obesity in older adults: A systematic review and meta-analysis. Clinical Nutrition *40*, 4633–4641. https://doi.org/10.1016/j.clnu.2021.06.009.

7. Luo, Y., Wang, Y., Tang, S., Xu, L., Zhao, X., Han, M., Liu, Y., Xu, Y., and Han, B. (2024). Prevalence of sarcopenic obesity in the older non-hospitalized population: a systematic review and meta-analysis. BMC Geriatr *24*, 357. https://doi.org/10.1186/s12877-024-04952-z.

8. Liu, C., Wong, P.Y., Chung, Y.L., Chow, S.K.-H., Cheung, W.H., Law, S.W., Chan, J.C.N., and Wong, R.M.Y. (2023). Deciphering the “obesity paradox” in the elderly: A systematic review and meta-analysis of sarcopenic obesity. Obesity Reviews *24*, e13534. https://doi.org/10.1111/obr.13534.

9. Benz, E., Pinel, A., Guillet, C., Capel, F., Pereira, B., De Antonio, M., Pouget, M., Cruz-Jentoft, A.J., Eglseer, D., Topinkova, E., et al. (2024). Sarcopenia and Sarcopenic Obesity and Mortality Among Older People. JAMA Netw Open *7*, e243604. https://doi.org/10.1001/jamanetworkopen.2024.3604.

10. Allen, J., Ramsden, M., and Nisar, S. (2024). Skeletal muscle structure, function and pathology. Orthopaedics and Trauma *38*, 137–144. https://doi.org/10.1016/j.mporth.2024.03.004.

11. McCuller, C., Jessu, R., and Callahan, A.L. (2026). Physiology, Skeletal Muscle. In StatPearls (StatPearls Publishing).

12. Structure of Skeletal Muscle | SEER Training https://training.seer.cancer.gov/anatomy/muscular/structure.html.

13. Song, J., Liu, J., Cui, C., Hu, H., Zang, N., Yang, M., Yang, J., Zou, Y., Li, J., Wang, L., et al. (2023). Mesenchymal stromal cells ameliorate diabetes-induced muscle atrophy through exosomes by enhancing AMPK/ULK1-mediated autophagy. J Cachexia Sarcopenia Muscle *14*, 915–929. https://doi.org/10.1002/jcsm.13177.

14. Lipina, C., and Hundal, H.S. (2017). Lipid modulation of skeletal muscle mass and function. J Cachexia Sarcopenia Muscle *8*, 190–201. https://doi.org/10.1002/jcsm.12144.

15. Yin, L., Li, N., Jia, W., Wang, N., Liang, M., Yang, X., and Du, G. (2021). Skeletal muscle atrophy: From mechanisms to treatments. Pharmacological Research *172*, 105807. https://doi.org/10.1016/j.phrs.2021.105807.

16. Reano, S., Graziani, A., and Filigheddu, N. (2014). Acylated and unacylated ghrelin administration to blunt muscle wasting. Current Opinion in Clinical Nutrition & Metabolic Care *17*, 236. https://doi.org/10.1097/MCO.0000000000000049.

17. Zhang, H., Qi, G., Wang, K., Yang, J., Shen, Y., Yang, X., Chen, X., Yao, X., Gu, X., Qi, L., et al. (2023). Oxidative stress: Roles in skeletal muscle atrophy. Biochemical Pharmacology *214*, 115664. https://doi.org/10.1016/j.bcp.2023.115664.

18. Saxton, R.A., and Sabatini, D.M. (2017). mTOR Signaling in Growth, Metabolism, and Disease. Cell *168*, 960–976. https://doi.org/10.1016/j.cell.2017.02.004.

19. Düvel, K., Yecies, J.L., Menon, S., Raman, P., Lipovsky, A.I., Souza, A.L., Triantafellow, E., Ma, Q., Gorski, R., Cleaver, S., et al. (2010). Activation of a metabolic gene regulatory network downstream of mTOR complex 1. Mol Cell *39*, 171–183. https://doi.org/10.1016/j.molcel.2010.06.022.

20. Ong, P.S., Wang, L.Z., Dai, X., Tseng, S.H., Loo, S.J., and Sethi, G. (2016). Judicious Toggling of mTOR Activity to Combat Insulin Resistance and Cancer: Current Evidence and Perspectives. Front Pharmacol *7*, 395. https://doi.org/10.3389/fphar.2016.00395.

21. Schiaffino, S., Dyar, K.A., Ciciliot, S., Blaauw, B., and Sandri, M. (2013). Mechanisms regulating skeletal muscle growth and atrophy. The FEBS Journal *280*, 4294–4314. https://doi.org/10.1111/febs.12253.

22. Bonaldo, P., and Sandri, M. (2013). Cellular and molecular mechanisms of muscle atrophy. Dis Model Mech *6*, 25–39. https://doi.org/10.1242/dmm.010389.

23. Li, F., Li, Y., Duan, Y., Hu, C.-A.A., Tang, Y., and Yin, Y. (2017). Myokines and adipokines: Involvement in the crosstalk between skeletal muscle and adipose tissue. Cytokine & Growth Factor Reviews *33*, 73–82. https://doi.org/10.1016/j.cytogfr.2016.10.003.

24. Ghesmati, Z., Rashid, M., Fayezi, S., Gieseler, F., Alizadeh, E., and Darabi, M. (2024). An update on the secretory functions of brown, white, and beige adipose tissue: Towards therapeutic applications. Rev Endocr Metab Disord *25*, 279–308. https://doi.org/10.1007/s11154-023-09850-0.

25. Harvey, I., Boudreau, A., and Stephens, J.M. (2020). Adipose tissue in health and disease. Open Biol *10*, 200291. https://doi.org/10.1098/rsob.200291.

26. Recinella, L., Orlando, G., Ferrante, C., Chiavaroli, A., Brunetti, L., and Leone, S. (2020). Adipokines: New Potential Therapeutic Target for Obesity and Metabolic, Rheumatic, and Cardiovascular Diseases. Front Physiol *11*, 578966. https://doi.org/10.3389/fphys.2020.578966.

27. Zamboni, M., Mazzali, G., Brunelli, A., Saatchi, T., Urbani, S., Giani, A., Rossi, A.P., Zoico, E., and Fantin, F. (2022). The Role of Crosstalk between Adipose Cells and Myocytes in the Pathogenesis of Sarcopenic Obesity in the Elderly. Cells *11*, 3361. https://doi.org/10.3390/cells11213361.

28. Park, M.J., and Choi, K.M. (2023). Interplay of skeletal muscle and adipose tissue: sarcopenic obesity. Metabolism *144*, 155577. https://doi.org/10.1016/j.metabol.2023.155577.

29. Larsson, L., Degens, H., Li, M., Salviati, L., Lee, Y. il, Thompson, W., Kirkland, J.L., and Sandri, M. (2019). Sarcopenia: Aging-Related Loss of Muscle Mass and Function. Physiol Rev *99*, 427–511. https://doi.org/10.1152/physrev.00061.2017.

30. Prado, C.M., Batsis, J.A., Donini, L.M., Gonzalez, M.C., and Siervo, M. (2024). Sarcopenic obesity in older adults: a clinical overview. Nat Rev Endocrinol *20*, 261–277. https://doi.org/10.1038/s41574-023-00943-z.

31. Adolph, T.E., and Tilg, H. (2024). Western diets and chronic diseases. Nat Med *30*, 2133–2147. https://doi.org/10.1038/s41591-024-03165-6.

32. Clemente-Suárez, V.J., Beltrán-Velasco, A.I., Redondo-Flórez, L., Martín-Rodríguez, A., and Tornero-Aguilera, J.F. (2023). Global Impacts of Western Diet and Its Effects on Metabolism and Health: A Narrative Review. Nutrients *15*, 2749. https://doi.org/10.3390/nu15122749.

33. Monsanto, S.P., Hintze, K.J., Ward, R.E., Larson, D.P., Lefevre, M., and Benninghoff, A.D. (2016). The new total Western diet for rodents does not induce an overweight phenotype or alter parameters of metabolic syndrome in mice. Nutrition Research *36*, 1031–1044. https://doi.org/10.1016/j.nutres.2016.06.002.

34. Wu, H., Flint, A.J., Qi, Q., van Dam, R.M., Sampson, L.A., Rimm, E.B., Holmes, M.D., Willett, W.C., Hu, F.B., and Sun, Q. (2015). Whole Grain Intake and Mortality: Two Large Prospective Studies in U.S. Men and Women. JAMA Intern Med *175*, 373–384. https://doi.org/10.1001/jamainternmed.2014.6283.

35. Wang, N.C., Bagheri, M., Olszewski, T., Friese, K.A., Smith, H.M., Robles, M.E., Wang, C., Brooks, A., Bordenstein, S.R., Ferguson, J.F., et al. (2021). New-Onset Vegetarian Diet Shows Differences in Fatty Acid Metabolites in European American and African American Women. Nutr Metab Cardiovasc Dis *31*, 2436–2448. https://doi.org/10.1016/j.numecd.2021.05.013.

36. Murru, E., Manca, C., Carta, G., and Banni, S. (2022). Impact of Dietary Palmitic Acid on Lipid Metabolism. Front. Nutr. *9*. https://doi.org/10.3389/fnut.2022.861664.

37. Annevelink, C.E., Sapp, P.A., Petersen, K.S., Shearer, G.C., and Kris-Etherton, P.M. (2023). Diet-Derived and Diet-Related Endogenously Produced Palmitic Acid: Effects on Metabolic Regulation and Cardiovascular Disease Risk. J Clin Lipidol *17*, 577–586. https://doi.org/10.1016/j.jacl.2023.07.005.

38. Murru, E., Manca, C., Carta, G., and Banni, S. (2022). Impact of Dietary Palmitic Acid on Lipid Metabolism. Frontiers in Nutrition *9*, 861664. https://doi.org/10.3389/fnut.2022.861664.

39. Paiella, M., Raiteri, T., Reano, S., Manfredelli, D., Manenti, T., Gentili, G., Meskine, H., Chiappalupi, S., Bellomo, G., Prodam, F., et al. (2025). Diet-Derived Advanced Glycation End-Products (AGEs) Induce Muscle Wasting In Vitro, and a Standardized Vaccinium macrocarpon Extract Restrains AGE Formation and AGE-Dependent C2C12 Myotube Atrophy. Antioxidants (Basel) *14*, 900. https://doi.org/10.3390/antiox14080900.

40. Ruiz, H.H., Ramasamy, R., and Schmidt, A.M. (2019). Advanced Glycation End Products: Building on the Concept of the “Common Soil” in Metabolic Disease. Endocrinology *161*, bqz006. https://doi.org/10.1210/endocr/bqz006.

41. Perrone, A., Giovino, A., Benny, J., and Martinelli, F. (2020). Advanced Glycation End Products (AGEs): Biochemistry, Signaling, Analytical Methods, and Epigenetic Effects. Oxidative Medicine and Cellular Longevity *2020*, 1–18. https://doi.org/10.1155/2020/3818196.

42. Mengstie, M.A., Chekol Abebe, E., Behaile Teklemariam, A., Tilahun Mulu, A., Agidew, M.M., Teshome Azezew, M., Zewde, E.A., and Agegnehu Teshome, A. (2022). Endogenous advanced glycation end products in the pathogenesis of chronic diabetic complications. Front. Mol. Biosci. *9*. https://doi.org/10.3389/fmolb.2022.1002710.

43. van Dongen, K.C.W., Kappetein, L., Miro Estruch, I., Belzer, C., Beekmann, K., and Rietjens, I.M.C.M. (2022). Differences in kinetics and dynamics of endogenous versus exogenous advanced glycation end products (AGEs) and their precursors. Food and Chemical Toxicology *164*, 112987. https://doi.org/10.1016/j.fct.2022.112987.

44. Twarda-Clapa, A., Olczak, A., Białkowska, A.M., and Koziołkiewicz, M. (2022). Advanced Glycation End-Products (AGEs): Formation, Chemistry, Classification, Receptors, and Diseases Related to AGEs. Cells *11*, 1312. https://doi.org/10.3390/cells11081312.

45. Fishman, S.L., Sonmez, H., Basman, C., Singh, V., and Poretsky, L. (2018). The role of advanced glycation end-products in the development of coronary artery disease in patients with and without diabetes mellitus: a review. Mol Med *24*, 59. https://doi.org/10.1186/s10020-018-0060-3.

46. Muthyalaiah, Y.S., Jonnalagadda, B., John, C.M., and Arockiasamy, S. (2021). Impact of Advanced Glycation End products (AGEs) and its receptor (RAGE) on cancer metabolic signaling pathways and its progression. Glycoconj J *38*, 717–734. https://doi.org/10.1007/s10719-021-10031-x.

47. Ott, C., Jacobs, K., Haucke, E., Navarrete Santos, A., Grune, T., and Simm, A. (2014). Role of advanced glycation end products in cellular signaling. Redox Biology *2*, 411–429. https://doi.org/10.1016/j.redox.2013.12.016.

48. Kang, R., Tang, D., Schapiro, N.E., Livesey, K.M., Farkas, A., Loughran, P., Bierhaus, A., Lotze, M.T., and Zeh, H.J. (2010). The Receptor for Advanced Glycation End-products (RAGE) Sustains Autophagy and Limits Apoptosis, Promoting Pancreatic Tumor Cell Survival. Cell Death Differ *17*, 666–676. https://doi.org/10.1038/cdd.2009.149.

49. Chiu, C., Yang, R., Sheu, M., Chan, D., Yang, T., Tsai, K., Chiang, C., and Liu, S. (2016). Advanced glycation end-products induce skeletal muscle atrophy and dysfunction in diabetic mice via a RAGE - mediated, AMPK -down-regulated, Akt pathway. The Journal of Pathology *238*, 470–482. https://doi.org/10.1002/path.4674.

50. Strieder-Barboza, C., Baker, N.A., Flesher, C.G., Karmakar, M., Neeley, C.K., Polsinelli, D., Dimick, J.B., Finks, J.F., Ghaferi, A.A., Varban, O.A., et al. (2019). Advanced glycation end-products regulate extracellular matrix-adipocyte metabolic crosstalk in diabetes. Sci Rep *9*, 19748. https://doi.org/10.1038/s41598-019-56242-z.

51. Gutowska, K., Czajkowski, K., and Kuryłowicz, A. (2023). Receptor for the Advanced Glycation End Products (RAGE) Pathway in Adipose Tissue Metabolism. Int J Mol Sci *24*, 10982. https://doi.org/10.3390/ijms241310982.

52. Unoki, H., Bujo, H., Yamagishi, S., Takeuchi, M., Imaizumi, T., and Saito, Y. (2007). Advanced glycation end products attenuate cellular insulin sensitivity by increasing the generation of intracellular reactive oxygen species in adipocytes. Diabetes Research and Clinical Practice *76*, 236–244. https://doi.org/10.1016/j.diabres.2006.09.016.

53. Feng, Z., Du, Z., Shu, X., Zhu, L., Wu, J., Gao, Q., Wang, L., Chen, N., Li, Y., Luo, M., et al. (2021). Role of RAGE in obesity-induced adipose tissue inflammation and insulin resistance. Cell Death Discov *7*, 305. https://doi.org/10.1038/s41420-021-00711-w.

54. Burattini, S., Ferri, P., Battistelli, M., Curci, R., Luchetti, F., and Falcieri, E. (2004). C2C12 murine myoblasts as a model of skeletal muscle development: morpho-functional characterization. Eur J Histochem *48*, 223–233.

55. Klein, A.J., and Vaughan, R.A. (2026). A Systematic Review and User Reference of Phenotypic and Molecular Characteristics of Dexamethasone-Mediated C2C12 Muscle Atrophy. J Cachexia Sarcopenia Muscle *17*, e70127. https://doi.org/10.1002/jcsm.70127.

56. Xu, X., Pang, Y., and Fan, X. (2025). Mitochondria in oxidative stress, inflammation and aging: from mechanisms to therapeutic advances. Sig Transduct Target Ther *10*, 190. https://doi.org/10.1038/s41392-025-02253-4.

57. Coll, T., Eyre, E., Rodríguez-Calvo, R., Palomer, X., Sánchez, R.M., Merlos, M., Laguna, J.C., and Vázquez-Carrera, M. (2008). Oleate Reverses Palmitate-induced Insulin Resistance and Inflammation in Skeletal Muscle Cells *. Journal of Biological Chemistry *283*, 11107–11116. https://doi.org/10.1074/jbc.M708700200.

58. Pratelli, G., Di Liberto, D., Carlisi, D., Emanuele, S., Giuliano, M., Notaro, A., De Blasio, A., Calvaruso, G., D'Anneo, A., and Lauricella, M. (2023). Hypertrophy and ER Stress Induced by Palmitate Are Counteracted by Mango Peel and Seed Extracts in 3T3-L1 Adipocytes. Int J Mol Sci *24*, 5419. https://doi.org/10.3390/ijms24065419.

59. de Hart, N.MMP., Petrocelli, J.J., Nicholson, R.J., Yee, E.M., Ferrara, P.J., Bastian, E.D., Ward, L.S., Petersen, B.L., Summers, S.A., and Drummond, M.J. (2023). Palmitate-Induced Inflammation and Myotube Atrophy in C2C12 Cells Are Prevented by the Whey Bioactive Peptide, Glycomacropeptide. J Nutr *153*, 2915–2928. https://doi.org/10.1016/j.tjnut.2023.08.033.

60. Lei, Y., Gan, M., Qiu, Y., Chen, Q., Wang, X., Liao, T., Zhao, M., Chen, L., Zhang, S., Zhao, Y., et al. (2024). The role of mitochondrial dynamics and mitophagy in skeletal muscle atrophy: from molecular mechanisms to therapeutic insights. Cell Mol Biol Lett *29*, 59. https://doi.org/10.1186/s11658-024-00572-y.

61. Rimessi, A., Previati, M., Nigro, F., Wieckowski, M.R., and Pinton, P. (2016). Mitochondrial reactive oxygen species and inflammation: Molecular mechanisms, diseases and promising therapies. The International Journal of Biochemistry & Cell Biology *81*, 281–293. https://doi.org/10.1016/j.biocel.2016.06.015.

62. Kyriakis, J.M., and Avruch, J. (2012). Mammalian MAPK signal transduction pathways activated by stress and inflammation: a 10-year update. Physiol Rev *92*, 689–737. https://doi.org/10.1152/physrev.00028.2011.